The structure of the complex of plastocyanin and cytochrome *f*, determined by paramagnetic NMR and restrained rigid-body molecular dynamics

Marcellus Ubbink[1†*], Mikael Ejdebäck[2], B Göran Karlsson[2] and Derek S Bendall[1]

Background: The reduction of plastocyanin by cytochrome *f* is part of the chain of photosynthetic electron transfer reactions that links photosystems II and I. The reaction is rapid and is influenced by charged residues on both proteins. Previously determined structures show that the plastocyanin copper and cytochrome *f* haem redox centres are some distance apart from the relevant charged sidechains, and until now it was unclear how a transient electrostatic complex can be formed that brings the redox centres sufficiently close for a rapid reaction.

Results: A new approach was used to determine the structure of the transient complex between cytochrome *f* and plastocyanin. Diamagnetic chemical shift changes and intermolecular pseudocontact shifts in the NMR spectrum of plastocyanin were used as input in restrained rigid-body molecular dynamics calculations. An ensemble of ten structures was obtained, in which the root mean square deviation of the plastocyanin position relative to cytochrome *f* is 1.0 Å. Electrostatic interaction is maintained at the same time as the hydrophobic side of plastocyanin makes close contact with the haem area, thus providing a short electron transfer pathway (Fe–Cu distance 10.9 Å) via residues Tyr1 or Phe4 (cytochrome *f*) and the copper ligand His87 (plastocyanin).

Conclusions: The combined use of diamagnetic and paramagnetic chemical shift changes makes it possible to obtain detailed information about the structure of a transient complex of redox proteins. The structure suggests that the electrostatic interactions 'guide' the partners into a position that is optimal for electron transfer, and which may be stabilised by short-range interactions.

Addresses: [1]Department of Biochemistry and Cambridge Centre for Molecular Recognition, University of Cambridge, Tennis Court Road, Cambridge CB2 1QW, England and [2]Department of Biochemistry and Biophysics, Göteborg University and Chalmers University of Technology, Lundbergslaboratoriet, Medicinaregatan 9C, S-413 90, Göteborg, Sweden.

[†]Present address: Leiden Institute of Chemistry, Leiden University, Gorlaeus Laboratories, P.O. Box 9502, 2300 RA Leiden, The Netherlands.

*Corresponding author.
E-mail: m.ubbink@chem.leidenuniv.nl

Key words: chemical shift, dynamic complex, electron transfer, photosynthesis, pseudocontact shift

Received: **30 October 1997**
Revisions requested: **5 December 1997**
Revisions received: **14 January 1998**
Accepted: **15 January 1998**

Structure 15 March 1998, **6**:323–335
http://biomednet.com/elecref/0969212600600323

Introduction

Cytochrome *f* and plastocyanin are two proteins involved in the photosynthetic electron transfer chain that links photosystems II and I. Cytochrome *f* is part of the cytochrome *bf* complex [1], which is located in the thylakoid membrane of chloroplasts. It has a large soluble N-terminal domain, anchored in the membrane by a single α helix [2]. The soluble domain (28.2 kDa) has an elongated shape and the single, covalently bound, haem group (*c*-type) is located in the middle of the protein and is coordinated by a histidine residue as well as the N-terminal amino group [3]. Cytochrome *f* acts as the natural reductant of plastocyanin, which is a soluble type I blue copper protein [4]. Crystal and solution structures of various plastocyanins have been published previously [5–11].

The cytochrome *f*–plastocyanin reaction is an excellent system for the study of interprotein electron transfer, because of its obvious physiological relevance and its high reaction rate ($2 \times 10^8\ M^{-1}s^{-1}$ at 25°C, 100 mM ionic strength, pH 6.0 [12]), despite the small driving force of about 20 mV [2,12] and the modest binding constant of about 7 mM^{-1} [12]. The latter presumably reflects a relatively high dissociation rate constant and the transient nature of the complex, which is necessary to maintain high rates of electron transfer under steady-state conditions. Kinetic measurements on unmodified [13–17], chemically modified [18–23] and genetically modified [12,24–27] forms of higher plant cytochrome *f* and plastocyanin indicate that the interaction between the two proteins is of a highly electrostatic nature *in vitro*. In a chemical crosslinking experiment, it was demonstrated that Asp44 (plastocyanin) can be linked to Lys187 (cytochrome *f*), suggesting that, at some stage in the complex formation, these residues are close to each other [28]. Another study showed that intracomplex electron transfer is severely inhibited by chemical crosslinking, which indicates that the initial complex may not be optimal for efficient electron transfer

and that rearrangement within the complex is necessary [29]. This theory is supported by kinetic evidence [17]. Recent *in vivo* measurements on cytochrome *f* variants in the green alga *Chlamydomonas reinhardtii*, with mutations that should affect the interaction with plastocyanin, showed only small effects on the growth rate and cytochrome photo-oxidation kinetics [30,31], which is surprising given the results of the *in vitro* studies. How the two can be reconciled remains as yet unclear.

Despite the substantial body of experimental results, it is still unresolved how plastocyanin binds to cytochrome *f*. In particular, the pathway used for electron transfer to the plastocyanin copper atom remains a matter of debate. Two pathways have been suggested: one via the hydrophobic patch, through the exposed copper ligand His87, the other via the acidic patch, through Tyr83 and copper ligand Cys84 (Figure 1). The latter patch is involved in the electrostatic interaction with cytochrome *f*, but the pathway through His87 appears to be the shorter. Determination of the structure of the soluble domain of cytochrome *f* revealed that it contains a positively charged site (lysine residues 58, 65, 66, 181 and 185, and arginine residues 184 and 209). This site is probably involved in the interaction with the acidic patch of plastocyanin (eight negative charges) and is not located close to the haem, suggesting that the haem area itself might interact with the hydrophobic patch. Two modelling studies [32,33] provide data that support this view.

In order to understand how rapid electron transfer is achieved in the transient complex of plastocyanin and cytochrome *f*, the structure of the complex was determined using a new approach, based on the changes in chemical shifts of plastocyanin nuclei upon binding to cytochrome *f*. By using both reduced and oxidized cytochrome *f*, it was possible to separate diamagnetic and paramagnetic contributions in the chemical shift changes. These data were used in restrained molecular dynamics calculations. The results indicate that plastocyanin binds in a single orientation to cytochrome *f*, with an interface that consists of both electrostatic and short-range interactions. The complex suggests a short electron transfer path from haem iron to the copper.

Results and discussion

Effects of complex formation

The complex of spinach plastocyanin and the soluble domain of turnip cytochrome *f* was determined using ^{1}H and ^{15}N NMR. The copper atom of plastocyanin was replaced by cadmium to create a redox-inactive plastocyanin substitute [34]. In order to observe solely the NMR signals of plastocyanin, this protein was enriched with ^{15}N, and ^{15}N-HSQC spectra were obtained to study the effects of complex formation. Upon addition of either reduced or oxidized cytochrome *f*, a general broadening of the resonances was observed and a number of peaks demonstrated chemical shift changes, indicating the formation of a complex between the two proteins. These effects were proportional to the fraction of bound plastocyanin and the line broadening of the shifted peaks was not larger than that of the other peaks, which showed that the complex was in fast exchange on the NMR timescale ($k_{off} >> 400\ s^{-1}$). An overlay of part of the ^{15}N-HSQC plastocyanin spectra of free plastocyanin, cytochrome *f*(II)–plastocyanin and cytochrome *f*(III)–plastocyanin is presented in Figure 2. Chemical shift changes observed in the cytochrome *f*(II)–plastocyanin complex vary from –0.11 to 0.06 ppm for protons and from –0.75 to 0.41 ppm for ^{15}N nuclei. Shifts are observed for residues in the hydrophobic patch as well as the acidic patch (Table 1), suggesting that both patches are involved in binding to cytochrome *f*. In the spectrum of the oxidized complex, some peaks show chemical shift changes that differ from the changes in the spectrum of the reduced complex, for example, Ser11 and Asp9 in Figure 2. As the only difference between the oxidized and the reduced complex is the oxidation state of the haem iron, this suggests that in the complex these plastocyanin residues are located close

Figure 1

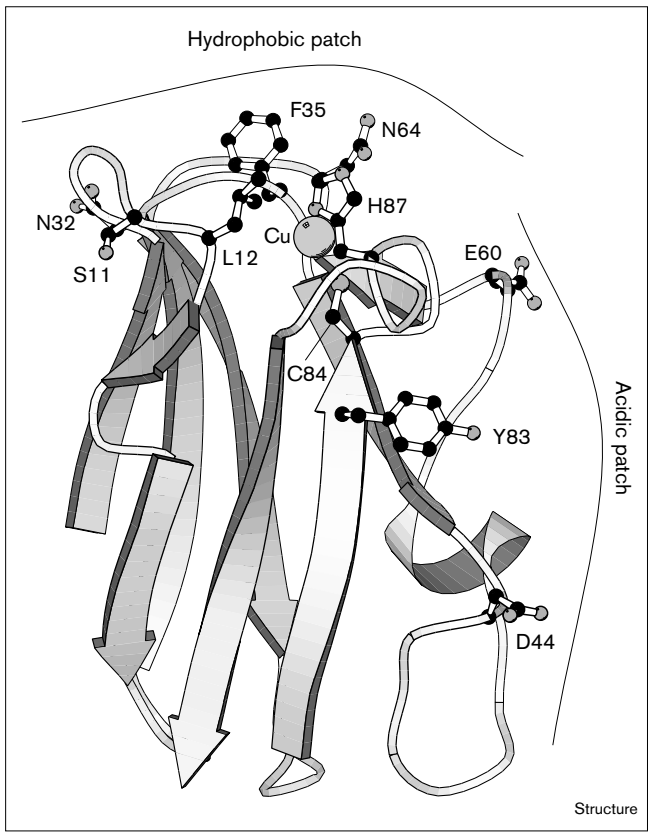

Backbone representation [75] of plastocyanin. Relevant residues are shown in ball-and-stick representation.

Figure 2

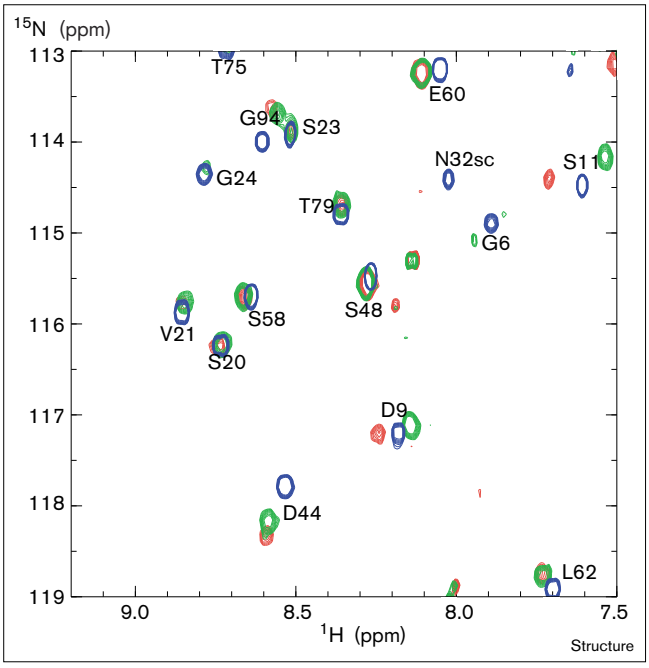

Overlay of part of the ^{15}N-HSQC spectra of free plastocyanin (blue), plastocyanin and reduced cytochrome *f* (green), and plastocyanin and oxidized cytochrome *f* (red). The cytochrome *f*:plastocyanin ratio was 0.8.

to the haem. The nuclei in these residues should experience intermolecular pseudocontact shifts in the oxidized complex because the Fe(III) is paramagnetic (spin = 1/2). Pseudocontact shifts have been exploited before for determination of the orientation of the magnetic susceptibility tensor and in structural studies [34–47]. While the present work was in progress, the use of intermolecular pseudocontact shifts was reported in a study of the complex of ferricytochrome b_5–ferricytochrome *c* [48].

Provided that the structure of the complex is the same in both oxidation states, the pseudocontact shift should be additional to the chemical shift change observed in the reduced complex (spin = 0):

$$\Delta\delta^{bin}(ox) = \Delta\delta^{bin}(red) + \Delta\delta^{pc} \quad (1)$$

in which $\Delta\delta^{bin}(ox)$ and $\Delta\delta^{bin}(red)$ are the chemical shift changes in the oxidized and reduced complexes caused by binding, respectively, and $\Delta\delta^{pc}$ is the pseudocontact shift. Table 1 lists the residues that demonstrated a significant pseudocontact shift $[\Delta\delta^{bin}(ox)–\Delta\delta^{bin}(red)]$. As the pseudocontact shift depends on the orientation and distance of a nucleus relative to the haem group but not on the gyromagnetic ratio, its sign and size should be similar for the ^{1}H and ^{15}N nuclei of any particular amide group. This is, in fact, the case for most residues that show significant changes for both nuclei (bold in Table 1). Only residues 87–89 appear to deviate significantly. The pseudocontact shifts range from –0.05 to 0.30 ppm and are observed solely for residues in the hydrophobic patch, indicating that in the complex this side of the plastocyanin is nearest to the haem.

Structure determination

The two categories of chemical shift changes, those caused by binding of plastocyanin to cytochrome *f* and the pseudocontact shifts, represent information about the structure of the complex. The former gives qualitative information about the sites that are part of the protein–protein interface, and the latter contains quantitative information about the orientation and distance of a number of plastocyanin nuclei relative to the haem iron. In order to convert this information into a model for the structure of the complex in an objective manner, restrained rigid-body molecular dynamics were performed. In this approach, both the structure of plastocyanin and cytochrome *f* are treated as rigid bodies by fixing the positions of the atoms within the molecule. In addition, cytochrome *f* was fixed, but plastocyanin was allowed to move relative to cytochrome *f* in order to search for an orientation that best fitted a set of restraints, as determined by minimization of an energy term. Low energy structures were subjected to restrained energy minimization in order to release van der Waals clashes and optimize sidechain orientation. Four groups of distance restraints were used, as well as one group of angle restraints.

Interface restraints

The first group, the interface restraints, consisted of nuclei that show a chemical shift ≥ 0.03 ppm (^{1}H) or ≥ 0.10 ppm (^{15}N) in the reduced complex compared with free plastocyanin (bold in Table 1). It was assumed that these nuclei are from residues that are part of the protein–protein interface and must therefore be within a certain distance of the cytochrome *f* surface (see Materials and methods for the details of the definition).

Pseudocontact restraints

The second group, the pseudocontact restraints, was based on the pseudocontact shifts. The size of the shift is described by [49]

$$\Delta\delta^{pc} = \frac{1}{24\pi r^3}\left(\left[2\chi_{zz}-(\chi_{xx}+\chi_{yy})\right]\left(3\cos^2\theta-1\right)+3\left(\chi_{xx}-\chi_{yy}\right)\sin^2\theta\cos 2\Omega\right) \quad (2)$$

in which χ_{ii} are the principal components of the magnetic susceptibility tensor and r, θ and Ω are the spherical coordinates of the nucleus in the coordinate system defined by the χ tensor. A number of approximations had to be made in order to use this relationship. The orientation of the susceptibility tensor relative to the crystal coordinate system of cytochrome *f* has not been reported. In other

Table 1

Significant chemical shift changes in plastocyanin nuclei upon binding to cytochrome *f*.

Residue	Δδ(red)* ppm		Δδ(ox)† ppm		Residue	Δδ(red)* ppm		Δδ(ox)† ppm	
	^{1}H ±0.02	^{15}N ±0.05	^{1}H ±0.03	^{15}N ±0.05		^{1}H ±0.02	^{15}N ±0.05	^{1}H ±0.03	^{15}N ±0.05
L4			**0.06**	**0.06**	S56		**−0.12**		
G6	**−0.04**		**0.08**	**0.11**	M57		**−0.13**		
G7	**−0.07**		**0.14**	**0.08**	S58	**0.03**			
D9	**−0.03**		**0.11**	**0.11**	E59	**0.04**	**0.12**	**−0.05**	**−0.08**
G10	**−0.05**	**−0.15**	**0.16**	**0.18**	E60	**0.06**			
S11	**−0.06**	**−0.28**	**0.19**	**0.28**	D61	**0.03**			
L12	**−0.07**		**0.30**	nd§	L62	**0.03**			−0.07
A13	**−0.07**	**−0.21**	**0.19**	**0.16**	N64		**−0.11**	0.07	0.19
L15			0.05	0.10	N64sc‡			**0.05**	**0.08**
E25				−0.08		**−0.04**		**0.04**	–
F29			0.03		G67			0.05	0.11
K30			0.06		E68			0.03	
N31			0.04	−0.08	Y70			0.03	
N32			**0.08**	**0.06**	K81		**−0.15**	nd§	nd§
N32sc‡		**0.11**	nd§	nd§	C84		**−0.15**	nd§	nd§
A33	**−0.05**		nd§	nd§	H87		**−0.64**	*0.12*	
F35		**−0.20**	**0.16**	**0.16**	Q88	**0.04**	**0.14**	*0.09*	*0.51*
H37			**0.10**	**0.10**	Q88sc‡	**0.05**	**−0.42**	**−0.05**	**−0.09**
N38	**−0.05**	**−0.16**	**0.07**	**0.07**		**−0.09**	–	**−0.08**	–
E43	**0.06**		−0.04	−0.11	G89		**−0.28**		*−0.20*
D44	**0.06**	**0.41**		0.06	A90	**−0.04**	**−0.75**	nd§	nd§
I46		**−0.28**		−0.07	G91		**−0.15**	**0.15**	**0.19**
A52				−0.07	M92	**−0.11**	**−0.23**	**0.18**	**0.10**
I55		**−0.13**			G94	**−0.05**	**−0.25**	0.03	
					K95		**0.11**		0.05

*Significant Δδ(red): ^{1}H ≥ 0.030; ^{15}N ≥ 0.100 ppm. †Significant Δδ(ox): ^{1}H ≥ 0.030; ^{15}N ≥ 0.050 ppm. Δδ(red) represents chemical shift changes for the reduced complex compared with free plastocyanin; Δδ(ox) represents chemical shift changes for the oxidized complex compared with the reduced complex. The values in bold have been used for the definition of the interface or pseudocontact restraints. Chemical shift differences for the oxidized complex were defined as pseudocontact shifts, if the ratio of ^{1}H:^{15}N shifts was between 0.5 and 2.0. The values in italics denote significant deviations from this definition. ‡sc = sidechain. §nd = not determined.

haem proteins, however, χ_{zz} is oriented nearly perpendicular to the haem plane [35–48], making a small angle with the bond between the iron and the sixth ligand. It was therefore assumed that χ_{zz} in cytochrome *f* is oriented along the bond between the iron and the N-terminal amino group. Because the values of the χ tensor components are also not known, the EPR-derived values for the g-tensor ($g_z = 3.51$, $g_y = 1.7$ and $g_x \leq 1.3$ [50,51]) were used instead. The fact that g_z is much larger than g_y and g_x suggests that the contribution of the term with $(\chi_{xx}-\chi_{yy})$ to the pseudocontact shift is relatively small and may be neglected. With these approximations Equation 2 converts into

$$\Delta\delta^{pc} = \frac{\mu_0\mu_B^2\, S(S+1)}{72\pi k T r^3}\left[2g_z^2 - \left(g_x^2 + g_y^2\right)\right]\left(3\cos^2\theta - 1\right) \qquad (3)$$

in which μ_0 is the permeability of vacuum ($4\pi \times 10^{-7}$ kg m s^{-1} A^{-2}), μ_B is the electron Bohr magneton (9.2741×10^{-24} J T^{-1}), S is the spin quantum number, *k* is the Boltzmann constant (1.3807×10^{-23} J K^{-1}) and T is temperature. Under the conditions used, plastocyanin in complex with cytochrome *f* is in fast exchange with the free form and spends about 55% of the time in the complex (based on the binding constant from an NMR titration at 45 mM ionic strength; results not shown). The pseudocontact shift is observed in the complex only and therefore $\Delta\delta^{pc}$ was multiplied by a factor *F* (occupancy fraction) that represents the percentage of plastocyanin bound. When T = 300K and S = 1/2, Equation 3 can be written as

$$\Delta\delta^{pc} = \frac{1.848 * 10^3 F}{r^3}\left(3\cos^2\theta - 1\right) \qquad (4)$$

in which $\Delta\delta^{pc}$ is given in ppm, r is the distance (Å) from the plastocyanin nucleus to the iron, θ is the angle between the nucleus, the iron and the nitrogen of the N-terminal amino group of cytochrome *f*. In the restrained rigid-body molecular dynamics, *F* was varied between various runs and gave the lowest energy structures for *F* = 0.2 rather than 0.55. This could be explained if the value of g_{ax} [$g_{ax} = g_z^2 - 0.5(g_x^2 + g_y^2)$], which is incorporated in the factor $1.848*10^3$, is smaller at 300K than the value calculated from the EPR data (10K). This effect has been observed for other *c*-type cytochromes [41]. Equation 4 was used to calculate target distances for all nuclei that showed pseudocontact shifts. As the target distance

depends on the orientation of plastocyanin relative to the haem (angle θ), the restraints were redefined regularly during the rigid-body molecular dynamics run, on the basis of the newest position of plastocyanin.

Minimal distance restraints

For all amide groups of which neither the ^{1}H nor the ^{15}N nucleus showed a pseudocontact shift, minimal distance restraints were defined (the third group). Given the angle θ, a distance can be calculated at which the pseudocontact shift would be smaller than the experimental error and thus would remain undetected. The nucleus had to be at this distance or further from the haem iron to satisfy the restraint.

Electrostatic restraints

The fourth group of distance restraints, electrostatic restraints, represents the electrostatic properties of the interaction between plastocyanin and cytochrome *f*. In a previous study [12], plastocyanin residues Asp42, Glu43, Asp44, Glu59 and Glu60 were shown to be involved in binding to cytochrome *f*. In the present work, it was assumed that these residues interact with the large positive patch on cytochrome *f*. Recent kinetic measurements *in vitro* on cytochrome *f* variants with mutations in this region support this hypothesis (XS Gong, personal communication). Restraints were defined for the Oδ1/ε1 atoms of these five negative residues, which were satisfied if these atoms were close to any one or several Nζ/η atoms of the lysine and arginine residues in the positive patch on cytochrome *f*.

Angle restraints

Finally, angle restraints were defined for the atoms that showed a pseudocontact shift. The sign of the pseudocontact shift depends on angle θ in Equation 4. For positive shifts, θ should be between 0° and 55°or between 125° and 180° and for negative shifts, θ should be between 55° and 125°.

Table 2

Restraint groups.

Restraint group	Type	No. of restraints	Scaling*	Number × scaling
Interface	distance	46	2	92
Pseudocontact	distance	36	20	720
Minimal distance	distance	79	5	395
Electrostatic	distance	5	100	500
Angle*	angle	36	–	–

*Scaling of the angle restraints is not comparable with that of distance restraints.

The restraint groups are listed in Table 2. In the molecular dynamics calculations, each group has a scaling factor. The product of the number of restraints and the scaling factor indicates the relative importance of each restraint group. Note that more weight was attached to the restraints based on the information from the quantitative pseudocontact shifts than from the qualitative binding effects.

Figure 3 shows the energy trace for the sum of the energy terms of all restraint categories (E_{tot}) for a representative run. Coordinates of the structures were recorded when E_{tot} fell below the threshold. The arrows indicate a random displacement of the plastocyanin molecule, which was executed when the molecule lingered in a high local

Figure 3

A representative restrained rigid-body molecular dynamics run. The energy term for all distance restraints (E_{tot}) is shown as a function of the cycle number. The arrows indicate the cycles in which a random displacement of plastocyanin occurred because E_{tot} was ≥ (5 × the threshold) and had not changed more than 20% over 10 cycles (≡ local minimum).

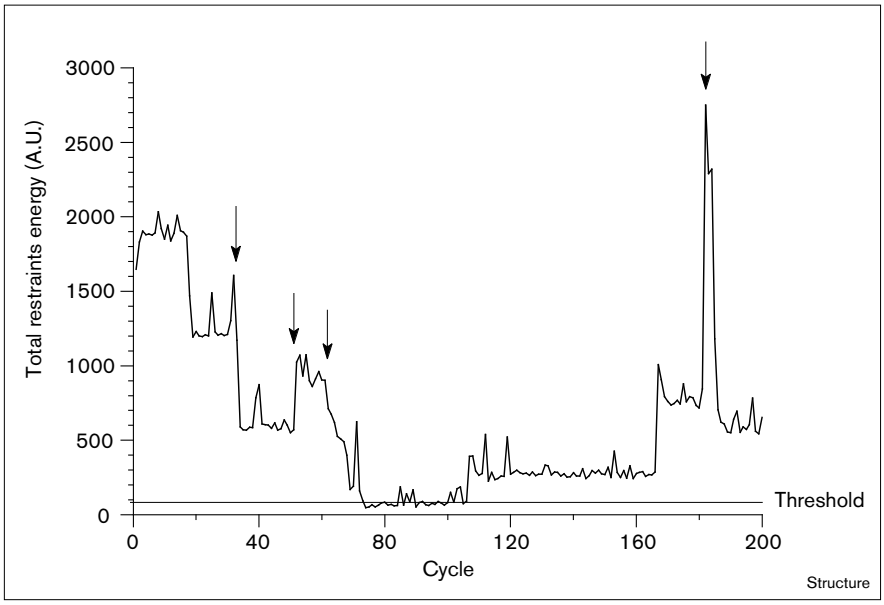

Figure 4

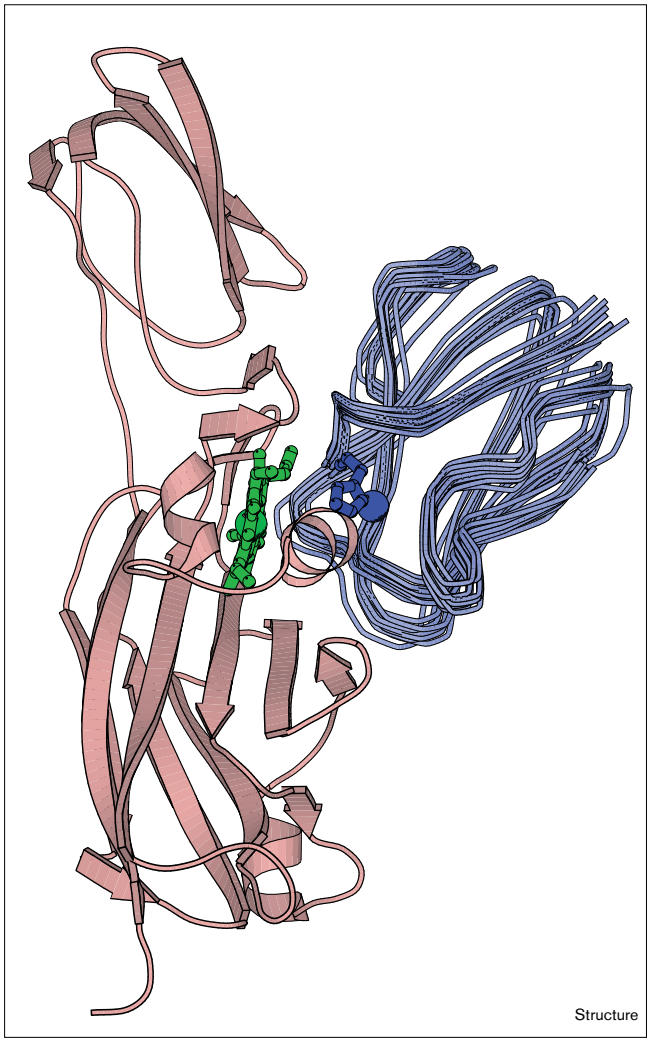

Ensemble of the ten lowest energy structures of the plastocyanin–cytochrome *f* complex. The positions of plastocyanin (Cα trace, in purple) relative to cytochrome *f* (pink) are shown for the ten structures with the lowest residual pseudocontact restraint energy after restrained energy minimization. The haem group (green) and His87 (blue) are shown in ball-and-stick representation; the copper atom is shown as a blue sphere.

minimum, $E_{tot} \geq (5 \times \text{threshold})$, for ten cycles. The structures with low energy all clustered close together. This behaviour was observed consistently and is independent of the starting position of plastocyanin.

Quality of the structure

The structures obtained from the restrained rigid-body molecular dynamics runs only showed violations of the interface and the pseudocontact restraints. The interface restraints represent qualitative information and the violations must be interpreted with some care (see below). An ensemble of the best ten structures therefore was obtained by selecting those with the lowest residual pseudocontact energy term. The ensemble, shown in Figure 4, clearly demonstrates that the data are in accordance with a single orientation for plastocyanin in the complex.

Accuracy of the structure

The accuracy of the structure depends on the quality of the method of determination, for which several points have to be considered. Firstly, in a molecular dynamics approach, it can never be excluded that other, equally good, solutions exist that simply have not been found. To diminish this chance, a considerable number of different starting positions for plastocyanin have been used in the molecular dynamics runs. No orientations for plastocyanin were found that had similarly low energies as that of the determined structure.

Secondly, systematic violations of the restraints may represent differences between the calculated and 'true' structure, because of limitations of the computational approach. No or very small violations were observed for the minimal distance restraints or the electrostatic restraints. The group of interface restraints showed systematic violations for a few amide nuclei. Some of these are found in residues located in the acidic patch (Ile46 and Ile55) and are part of the interface. Despite this fact, these nuclei still cause violations because cytochrome *f* backbone atoms, rather than surface atoms, had to be used for the definition of the interface restraints (see Materials and methods) and in this part of cytochrome *f* the surface is relatively far from the backbone. The violations of a few other nuclei appear to represent the transmitted effects of complex formation onto the protein (Gly6 NH and Asn32 Nδ2 via interface residue Leu12, and the amides of residues 94–96 via the interface residues around A90). Figure 5a shows that all backbone angle restraints are satisfied, indicating that the orientation of plastocyanin must be close to the 'true' one. The violations for the pseudocontact restraints were evaluated by back-calculation as demonstrated in Figure 5b for the ensemble of structures. This is more informative than determining distance violations, because these become disproportionately high for some values of θ (Equation 3) and they do not reflect the sign of the pseudocontact shift. It is clear from Figure 5b that the structure has some residual violations of the pseudocontact restraints. The pseudocontact restraints had to be calculated on the basis of several approximations concerning the χ-tensor. The target distances and angles were defined loosely to take into account errors in the orientation in the χ_{zz} and size of g_{ax} as well as errors due to the neglected $(\chi_{xx}–\chi_{yy})$ term. To allow for an error in the value of the g_{ax}, the occupancy fraction *F* was varied systematically. For a value of 0.1, plastocyanin tended to collide with cytochrome *f*, because it is pulled too close to the haem. For 0.3 and 0.4, plastocyanin moved away from the haem, creating a gap between the hydrophobic patch and the haem region, which is not in agreement with the observed diamagnetic chemical shift

Figure 5

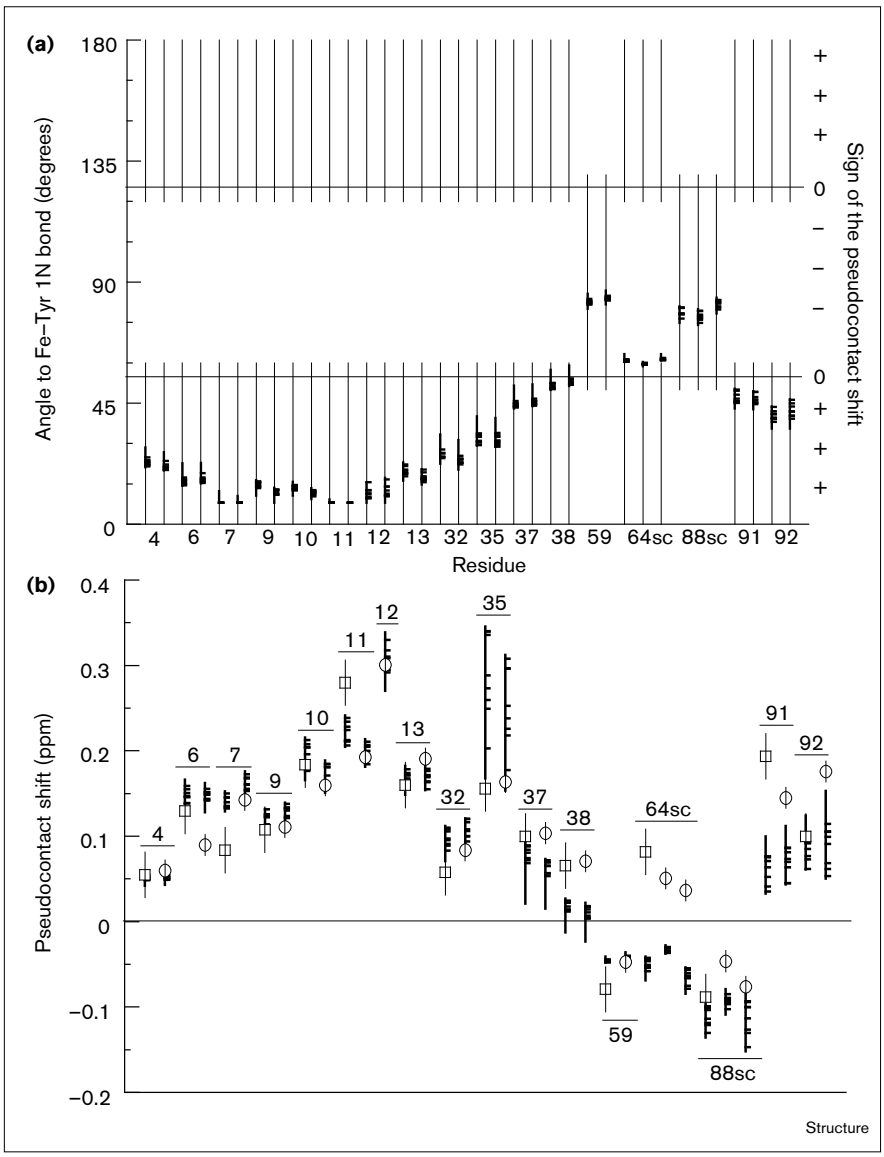

Angle and pseudocontact restraint violations. **(a)** The angles formed by a given nucleus, the haem iron atom and Tyr1 N atom is shown for ^{15}N (left) and NH (right) of residues that demonstrate a pseudocontact shift (Table 1). The angles of all ten structures of the low energy ensemble are given as 'high-low' symbols (vertical bar plus horizontal dashes). 64sc and 88sc represent the sidechain amides (^{15}N, ^{1}H, ^{1}H) of Asn64 and Gln88, respectively. The thin vertical bars indicate the target regions, based on the sign of the pseudocontact shifts and error margins. **(b)** The back-calculated pseudocontact shifts for the ten structures of the low energy ensemble are shown by the 'high-low' symbols. The experimentally observed pseudocontact shifts are represented by the open symbols (square, ^{15}N; circle, NH). Residue numbers are given. Note that in the ensemble the pseudocontact shifts of the sidechain amide of Asn64 have the wrong sign. In the energy minimization, the sidechain was rotated to relieve the angle restraint violation, but only until the angle reaches the error margin, as shown in (a). Under that specific condition, no angle restraints exist to rotate the sidechain further and the distance restraints are ineffective because the sign is wrong, thus causing the observed violation.

changes in the hydrophobic patch; these suggest that intimate contact exists between plastocyanin and cytochrome *f*. Therefore, F = 0.2 gave the best results. The fact that some violations remain, suggests that the approximated description of the χ-tensor is the factor that limits the accuracy of the structure.

Finally, in the molecular dynamics runs both proteins were treated as rigid bodies, thus allowing no changes in the positions of sidechains. In the restrained energy minimizations, only those sidechains moved that had van der Waals collisions or did not satisfy restraints. Because no solvent was present and electrostatics were not taken into account, the surface complementarity in the structure will not be optimal.

Precision of the structure

To assess the precision of the structure, it is most relevant to determine how precisely the position of plastocyanin is defined relative to that of cytochrome *f*. The procedure of rigid-body molecular dynamics, followed by energy minimization, is implicitly based on the hypothesis that the structures of both proteins remain largely unchanged upon complex formation. It is therefore useful to distinguish between a 'fitted root mean square deviation (rmsd)' and a 'positional rmsd'. The fitted rmsd is the rmsd obtained after superposition of the two structures that are being compared. The average fitted rmsds for the ensemble of structures compared with the mean structure are 0.004 Å and 0.048 Å for the backbone and all non-hydrogen atoms of cytochrome *f*, respectively. For plastocyanin, these

Figure 6

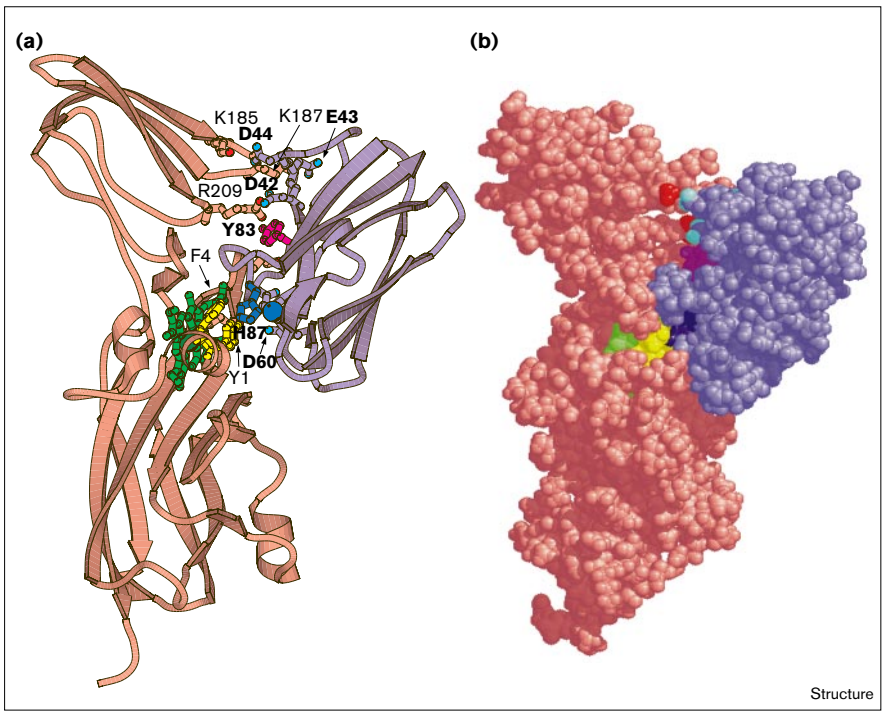

The structure of the plastocyanin–cytochrome *f* complex. The structure of the complex is shown with plastocyanin in purple and cytochrome *f* in orange in **(a)** backbone and **(b)** spacefilling representations, shown in identical orientations. The color coding is green, haem; yellow, Tyr1 and Phe4; red, Nζ and Nη atoms of Lys185, Lys187 and Arg109; dark blue, His87 and copper; magenta, Tyr83; cyan, Oδ/ε atoms of Asp42, Glu43, Asp44 and Asp60. Plastocyanin residues are indicated in bold text.

values are 0.198 Å and 0.130 Å. These numbers merely indicate that the overall structure of both molecules is maintained during energy minimization. The positional rmsd is the rmsd obtained for two structures that are not superimposed. The average positional rmsd for the plastocyanin structures in the ensemble (Figure 4) compared to the mean plastocyanin structure is a measure of the precision of the structure of the complex. This is 1.05 Å for all non-hydrogen atoms. It is concluded that the number of restraints was sufficient to produce convergence to a well-defined structure.

Description of the structure

Figure 6 shows the structure of the complex in backbone and spacefilling representations. Both the hydrophobic and acidic patch of plastocyanin make contact with the cytochrome *f* surface, with a total interface size of 400–500 Å^2. Plastocyanin residues Asp42, Glu43 and Asp44 are close to cytochrome *f* residues Arg209, Lys187 and Lys185, respectively, and residues Glu59 and Glu60 are close to Lys65 and Lys58, respectively. Plastocyanin residue Asp51 was not restrained, yet it is close to Lys187. Glu45 and Asp61 are not close to positive groups on cytochrome *f*, but it cannot be concluded that these residues have no role in the electrostatic interaction. These residues were not used in the electrostatic restraint list and electrostatic interactions were not included directly in the calculations, so simply no force acted upon them. In plastocyanin, the hydrophobic patch residues Gly10, Leu12, Phe35, Pro36, Leu62, Asn64 and Ser85–Ala90 are close (< 4 Å) to cytochrome *f* atoms. A very short electron transfer pathway is present from the haem to the copper atom, because the copper ligand His87 makes van der Waals contact with cytochrome *f* residues Phe4 and the haem ligand Tyr1 (Figure 7). The shortest distance is found between His87 Nε2 and Tyr1 Cδ2 (average distance 2.9 Å). The copper–iron distance ranges from 10.7 to 11.3 Å with an average of 10.9 Å. This strongly suggests that electron transfer proceeds via His87. Earlier studies, based on kinetic measurements on plastocyanin mutants Tyr83→Phe and Tyr83→Leu [24–26], had suggested that Tyr83 was part of the route used for electron transfer; these results are currently being re-evaluated.

In a set of six plastocyanin–cytochrome *f* complexes obtained via electrostatic calculations and molecular dynamics [33] one is similar, though not identical, to the experimentally based structure reported here. The coordinates, of this structure (denoted D; GM Ullmann, personal communication) were used for backcalculation of the pseudocontact shifts and to determine the restraint violations. It produced an E_{tot} that is below the threshold used in the rigid-body molecular dynamics and would therefore have been considered a low energy structure. The structure, however, is not in complete agreement with the experimental data, as judged by restraint violations in several restraint groups. Although the N-terminal plastocyanin loop in the hydrophobic patch is far from the

Figure 7

A short electron transfer pathway. Stereodiagram showing the copper atom of plastocyanin, His87 (the copper ligand), cytochrome *f* residue Phe4 and the haem group with ligands Tyr1 and His25. The plastocyanin residue His87 is shown in bold lines.

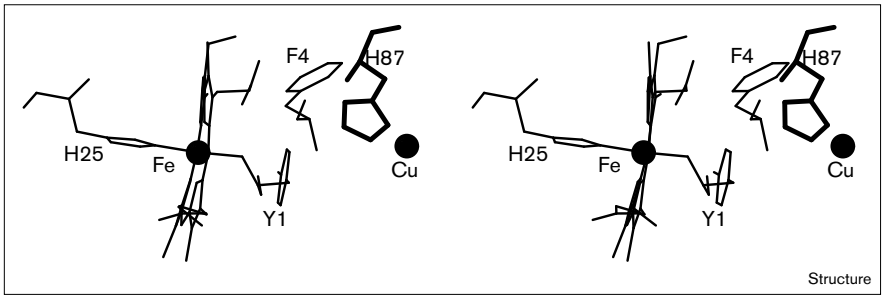

surface of cytochrome *f*, considerable chemical shift changes are observed for nuclei in that loop. Some of the backcalculated pseudocontact shifts are much too high, suggesting that the orientation of plastocyanin relative to haem is not completely correct, and the electrostatic interactions with the cytochrome *f* area around Lys65 appear to be poor. The iron–copper distance is larger in this theoretical structure (13.6 Å) and a route for electron transfer is less obvious. The experimental structure reported here also resembles a manually docked complex (complex number *2* reported in [32]).

A two-step model for complex formation

Kinetic measurements [17] and crosslinking studies [29] have suggested that the initial electrostatic binding of plastocyanin to cytochrome *f* does not result in a complex that is optimal for the electron transfer and that internal rearrangement is necessary. The basis for the structure of the complex presented in this study is a set of NMR data. In principle, these could represent a single complex or the average of an ensemble of complexes, which are in fast exchange. A large ensemble of very different orientations, however, is unlikely, because then the pseudocontact shifts would tend to average out, as observed in the complex of plastocyanin and cytochrome *c* [52]. If there were more than one plastocyanin orientation in the complex, it would be likely that these would affect the chemical shifts in acidic and hydrophobic patches to a different degree. A titration of the ^{15}N-HSQC spectra of the oxidized and reduced complexes between 10 and 70 mM ionic strength, however, did not show any differentiation of the chemical shift changes into groups. With increasing ionic strength, all chemical shift changes decreased with the same ratio, which is due to a decreasing binding constant (results not shown). Also a temperature titration of the HSQC spectra between 289 and 307K did not show any differentiation. This strongly suggests that the NMR data represent a single structure, rather than an average of several structures.

To resolve this paradox with the kinetic and crosslinking data, which suggest the presence of at least two structures, the following two-step model for the formation of an electrostatic complex is proposed (Figure 8). The first complex formed (Figure 8b; B) is of purely electrostatic nature, because the electrostatic interaction is active over long distances, whereas other non-covalent interactions are short-range forces. This complex would consist of a set of complexes, as Brownian dynamics calculations [53] have shown that within purely electrostatic complexes, multiple orientations of similar energy levels normally coexist. Recent electrostatic calculations for the plastocyanin–cytochrome *f* complex have demonstrated this quite clearly as well [33]. These complexes would be relatively 'loose' and no water exclusion from the interface area is likely to occur. Rapid exchange between various electrostatic orientations would therefore be possible. These features would result in very small diamagnetic chemical shift changes and cancellation of any intermolecular pseudocontact shifts. Rates of electron transfer would also be very low because of the strong decay of electronic coupling with distance, especially in the case of 'through

Figure 8

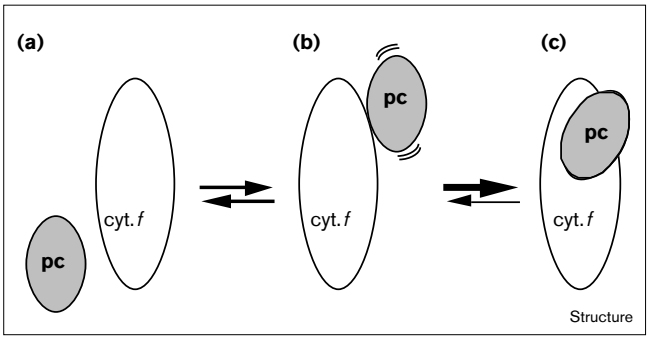

Model for the formation of an electrostatic complex. **(a)** Free proteins, **(b)** ensemble of 'loose' structures based on electrostatic interactions, which are in fast exchange, and **(c)** single, tighter, binding site, based on electrostatic as well as short-range forces. In the complex of plastocyanin (pc) and cytochrome *f* (cyt.*f*), the equilibrium between (b) and (c) is to the right, whereas in the plastocyanin–cytochrome *c* complex it is to the left [52].

space' coupling, which has been calculated to cause rates to decay by a factor of ten for every additional 1.4 Å [54,55]. The second step is the formation of a well-defined single-orientation complex (Figure 8c; C). Hydrogen bonding, hydrophobic interactions and van der Waals contacts all contribute to the binding energy. There would be fast exchange between forms B and C, shown in Figures 8b and c. The position of the equilibrium depends on the system under study. The data on the plastocyanin–cytochrome *c* complex suggest that in this case the equilibrium is strongly towards form B, because the chemical shift changes are very small and no pseudocontact shifts are observed [52]. In the case of plastocyanin and cytochrome *f*, the equilibrium appears to be to the right, given the larger chemical shift changes and the presence of pseudocontact shifts. The optimum in the electron transfer rate as a function of ionic strength [17] could be interpreted as an equilibrium shift from C to B at very low ionic strength.

According to this model, short-range forces are only effective in form C, but the relative importance of electrostatic forces in the two forms of the complex cannot yet be accurately assessed. General arguments suggest that electrostatics contribute substantially to form C, consistent with the structure we have determined. Nevertheless, the electrostatic restraints used in our molecular dynamics modelling were deduced from kinetic results and not from direct observation by NMR. In order to determine the influence of these restraints on the resulting structure, rigid-body molecular dynamics runs were performed in which the electrostatic restraints were left out and more weight was attached to the interface restraints, relative to the paramagnetic restraints. The lowest energy structures of the complex that were obtained show plastocyanin in essentially the same orientation as in Figure 4. Several other orientations with somewhat higher energy were also found. The electrostatic restraints therefore appear to single out one of the orientations and help to define this one with better precision. In terms of the two-step model, we conclude that some electrostatic interactions are retained in form C, and that their role is to guide the partners into a position that is optimal for electron transfer and which is further stabilized by short-range interactions.

This model could also explain why in crosslinked complexes, no electron transfer is observed. When the proteins are crosslinked in the presence of 1-ethyl-3-(2-dimethylaminopropyl) carbodiimide at pH 6.5, the reaction is normally carried out at low ionic strength to encourage formation of the electrostatic complex. Although the crosslink involves covalent contact, the groups concerned are unlikely to be favourable for electron transfer and one of the orientations of form B will be selected. As discussed above, these are optimized electrostatically, but not for electron transfer. It may be significant that Lys187 of cytochrome *f* and Asp44 of plastocyanin, which have been shown to undergo crosslinking [28], are not in close contact in form C.

The concept of rearrangement between two different forms of complex, as proposed here, has become a common theme of studies of biological electron transfer reactions, for example between yeast cytochrome *c* and cytochrome *c* peroxidase [56], methylamine dehydrogenase and amicyanin [57], cytochrome *c* and cytochrome *c* oxidase [58] and cytochrome c_2 and the photosynthetic reaction centre of purple bacteria [59]. Similar models have been proposed for the non-physiological reactions between the photo-excited Zn-porphyrin form of cytochrome *c* and plastocyanin [60] or cytochrome b_5 [61]. Protein–protein interactions in the two forms of the complex probably involve overlapping sites or a single binding domain [62]. Independent sites seem to be uncommon, although there is clear evidence for two independent sites in the case of cytochrome *c* peroxidase binding cytochrome *c* [62]. The kinetic evidence supporting rearrangement provides little information about the nature of the two forms of complex. The existence of an ionic strength optimum in several systems indicates that electrostatic forces favour one form (the less reactive one) over the other. The more reactive form of the complex would involve close protein–protein contacts and exclusion of water, as discussed in more detail elsewhere [63], but some electrostatic interaction will probably be retained. In this context, the importance of the work described here is twofold. Firstly, it provides experimental evidence of a specific structure for the more stable (and probably more reactive) form of the complex between cytochrome *f* and plastocyanin (C; Figure 8c), and it shows that both hydrophobic and electrostatic effects can be involved simultaneously. Secondly, the initial purely electrostatic form (B), the existence of which is implied by other work, lacks associated paramagnetic shifts and therefore must be dynamic, with numerous orientations in fast exchange with each other. In the case of cytochrome *c* and cytochrome *c* peroxidase, the kinetics of such multiple conformations have been observed with a fluorescence quenching technique by freezing them out at 77K [64]. This, and other experiments, led McLendon to propose the 'Velcro' model, according to which the initial recognition between soluble redox partners is not by a stereospecific lock-and-key interaction, but by one involving complementary charged patches which can associate in many different orientations of similar energy like pieces of Velcro material [65–67]. The dynamic nature of the initial electrostatic complex has also been successfully modelled by Brownian dynamics simulations [53], whereas information concerning the close forms of complexes is scarce.

Finally, we should stress that our results relate to the interaction between plastocyanin and a soluble form of

cytochrome *f in vitro*, albeit under conditions of pH and ionic strength not too dissimilar from those that may occur in the thylakoid lumen. In the intact thylakoid, the native form of cytochrome *f* is anchored to the membrane and plastocyanin may undergo a two-dimensional diffusion over the membrane surface rather than a three-dimensional diffusion in the lumen space [68]. Nevertheless, our conclusions regarding the complex between these two protein are based upon their detailed structure and physico-chemical properties and hence are likely to be relevant to the situation *in vivo*.

Biological implications

The reduction of plastocyanin, a water-soluble copper protein, by cytochrome *f*, a component of the cytochrome *bf* complex, is a central reaction of the photosynthetic electron transport chain of most oxygenic organisms. Electron transfer reactions are involved not only in photosynthesis but also in respiration and a range of other metabolic processes. Reactions between redox partners, in which either or both are diffusible proteins that must form a transient complex for the reaction to occur (as is the case for plastocyanin–cytochrome *f*), are less well understood than those within a protein or stable protein complex. This is largely because of the lack of precise structural information about the reactive state of the complex. We describe the results of a novel application of NMR spectroscopy which form the basis for use in restrained molecular dynamics calculations, to obtain the structure of the complex formed between a large water-soluble fragment of cytochrome *f* and plastocyanin. A single structure, which provides a short electron-transfer path between the haem group of cytochrome *f* and copper atom of plastocyanin, was obtained under a variety of experimental conditions. In contrast, kinetic measurements and crosslinking studies have suggested that initial electrostatic binding of plastocyanin to cytochrome *f* does not result in a complex that is optimal for electron transfer and so internal rearrangement is required. In order to reconcile our result with previous kinetic observations and crosslinking experiments, a two-step model for formation of the complex is proposed in which a dynamic, purely electrostatic, complex with many rapidly exchanging orientations is formed first and is then rapidly converted, under the influence of short-range forces, into a single, more specific, structure. This model of the reaction process is similar to those that have been proposed to explain other electron transfer reactions, especially between cytochrome *c* and cytochrome *c* peroxidase in yeast mitochondria. Our results therefore contribute to a general understanding of the role of electrostatics and short-range forces in interprotein electron transfer. The distinctive feature of these results is the use of NMR to obtain detailed structural information about the complex formed, and the technique described is probably applicable to other systems involving formation of transient complexes.

Materials and methods

Sample preparation

Spinach plastocyanin enriched with ^{15}N was produced in *Escherichia coli*, grown on M9 minimal medium [69] containing $^{15}NH_4Cl$ as nitrogen source. The protein was purified as previously described [70]. Cadmium substitution was performed according to a previously used method [34]. The soluble domain of cytochrome *f* from turnip was purchased from Sigma. NMR samples contained 1.0 mM plastocyanin and 0.8 mM cytochrome *f* in 90% buffer (5 mM potassium phosphate and 39 mM sodium chloride) and 10% D_2O and had an ionic strength of 40 mM (pH 6.0). The concentration determinations were based on optical spectra using $\varepsilon_{554} = 31.5\ mM^{-1}\ cm^{-1}$ for cytochrome *f* in the reduced form, $\varepsilon_{597} = 4.7\ mM^{-1}\ cm^{-1}$ for oxidized plastocyanin and $\varepsilon_{277} = 5.8\ mM^{-1}\ cm^{-1}$ for Cd–plastocyanin. Cytochrome *f* was kept in a reduced form with a few equivalents of sodium ascorbate and was stable in this form for days. The oxidized form showed a tendency to precipitate as well to autoreduce. The rate of autoreduction appeared to differ between cytochrome *f* batches. NMR spectra of free plastocyanin, the reduced complex and the oxidized complex were always taken on the same sample. Either oxidized cytochrome *f* was added to the plastocyanin and later reduced with ascorbate or reduced cytochrome *f* was added and later oxidized with half a molar equivalent of H_2O_2. Both approaches gave the same results.

NMR experiments and analysis

NMR experiments were performed on a Bruker AM500 (Cambridge), a Varian Unity 500 MHz (Göteborg) and a Varian Unity plus 600 MHz spectrometer (Swedish NMR Centre, Stockholm). All measurements, except the temperature titration, were performed at 300K.

^{15}N-HSQC spectra were obtained according to [71] with spectral widths of 20.7 ppm (^{15}N) and 13.3 ppm (^{1}H) and 128 and 1024 complex points in the indirect and direct dimensions, respectively. Data processing was performed with AZARA (available from: ftp://ftp.bio.cam.ac.uk/pub/azara/) and data analysis with Ansig [72, 73]. Proton and ^{15}N assignments of reduced spinach plastocyanin were kindly provided by A Bergkvist. With these, assignments of the Cd-substituted spinach plastocyanin could be made readily on the basis of the chemical shift changes observed for cadmium-substituted pea plastocyanin, as compared to its reduced form [34].

Structure determination

Restrained rigid-body molecular dynamics and restrained energy minimization were performed with X-PLOR version 3.1 [74]. The various restraint groups were defined in the following way. The interface restraints were set up as distance restraints between a particular plastocyanin nucleus and all backbone amide N atoms of cytochrome *f*, using the r^{-6} averaging option. Because of this averaging procedure, the restraint is satisfied only when the nucleus gets close to a single or a few cytochrome *f* N atoms; N atoms further away hardly contribute to the averaged distance to the plastocyanin nucleus. The advantage of this approach is that a restraint is obtained that attracts the nucleus non-specifically to cytochrome *f*. However, the N atoms represent the backbone, rather than the surface; where the surface is far from the backbone, the plastocyanin nucleus cannot fully satisfy the restraint, even though it may be in contact with the surface, as observed for nuclei in the acidic patch (see above). The target of the square-well function was 16 and 11 Å for plastocyanin backbone and sidechain amide nuclei, respectively. The electrostatic restraints were defined in the same way, except that the r^{-6} averaging was done over the distances to the cytochrome nuclei Nζ or Nη1 of lysine residues 58, 65, 66, 181, 185 and 187, and arginine residues 184 and 209, and a target of 6.5 Å.

The definition of the pseudocontact restraints has been described above. A square-well function was used and the target was redefined

after each cycle of 1000 steps. The angle restraints for the angle of a plastocyanin nucleus with the bond between the iron and the N-terminal amino group were defined as dihedral restraints for the dihedral between the plastocyanin nucleus–haem atom NB vector and iron–amino bond. The target dihedral was set to the target angle and adjusted for the difference between the actual angle and dihedral. This difference varies with the orientation of plastocyanin and therefore the restraint was redefined after each cycle.

In the rigid-body molecular dynamics no other energy terms were used apart from the restraint terms. van der Waals collision was (largely) prevented by a set of 55 distance restraints for plastocyanin nuclei spread evenly over the molecule, which were defined in the same way as the interface restraints, but used a high scaling factor and an exponent of 4 (all other restraints used 2). This approach proved more stable than any of the van der Waals functions available. The step time was 40 fs and a run of 200 cycles is 8 ns. However, as only restraint energy terms were used, this number has no physical meaning. The temperature was set to 5000K, using the TBATH option in X-PLOR, but it showed large fluctuations. The general scaling factor for the restraints was 0.008 and the threshold for saving coordinates was 80. A run of 200 cycles took 7.5 hrs CPU time on a Silicon Graphics Indigo2.

Restrained energy minimization (Powell option) was performed using the bond, angle, dihedral, improper and van der Waals energy terms, as well as all the restraints mentioned above, except for the 55 restraints that prevented collisions. The target for the electrostatic restraints was set to 4 Å. An extra set of 45 distance restraints was defined using a square-well function with a narrow well and high exponent and scale for nuclei within plastocyanin, in order to maintain the overall structure of this protein without fixing any coordinates. The position of cytochrome *f* was fixed by fixing the positions of the C′ atoms in the backbone. The energy minimisation continued for 10 cycles of 200 steps.

Accession numbers

The coordinates of the ensemble of 10 plastocyanin molecules and cytochrome *f* have been deposited at the Protein Data Bank under accession number 2PCF.

Acknowledgements

The authors would like to thank A Bergkvist for providing the assignments and the solution structure of spinach plastocyanin before publication, and GM Ullmann (Free university, Berlin) for kindly providing coordinates of cytochrome *f*–plastocyanin complexes, obtained by molecular dynamics. C Damberg and A Öhman of the Swedish NMR centre (Stockholm; now Swedish NMR Centre at Göteborg University) are acknowledged for the help with the NMR measurements. ARC Raine is acknowledged for his help with the molecular dynamics. This work was supported by the Biotechnology and Biological Sciences Research Council (UK), the Swedish Natural Science Research Council and the European Science Foundation, which has provided a short-term fellowship to MU in the programme Biophysics of Photosynthesis.

References

1. Cramer, W.A., *et al*., & Smith, J.L. (1996). Some new structural aspects and old controversies concerning the cytochrome b_6f complex of oxygenic photosynthesis. *Annu. Rev. Plant Physiol. Plant Mol. Biol.* **47**, 477-508.
2. Gray, J.C. (1992). Cytochrome *f*: structure, function and biosynthesis. *Photosynthesis Res.* **34**, 359-374.
3. Martinez, S.E., Huang, D., Szczepaniak, A., Cramer, W.A. & Smith, J.L. (1994). Crystal structure of chloroplast cytochrome *f* reveals a novel cytochrome fold and unexpected heme ligation. *Structure* **2**, 95-105.
4. Canters, G.W. & Gilardi, G. (1993). Engineering type 1 copper sites in proteins. *FEBS Lett.* **325**, 39-48.
5. Guss, M.J. & Freeman, H.C. (1983). Structure of oxidized poplar plastocyanin at 1·6 Å resolution. *J. Mol. Biol.* **169**, 521-563.
6. Collyer, C.A., Guss, J.M., Sugimura, Y., Yoshizaki, F. & Freeman, H.C. (1990). Crystal structure of plastocyanin from a green alga, *Enteromorpha prolifera*. *J. Mol. Biol.* **211**, 617-632.
7. Moore, J.M., Lepre, C.A., Gippert, G.P., Chazin, W.J., Case, D.A. & Wright, P.E. (1991). High-resolution solution structure of reduced french bean plastocyanin and comparison with the crystal structure of poplar plastocyanin. *J. Mol. Biol.* **221**, 533-555.
8. Guss, J.M., Bartunik, H.D. & Freeman, H.C. (1992). Accuracy and precision in protein structure analysis: restrained least-squares refinement of the structure of poplar plastocyanin at 1.33 Å resolution. *Acta Cryst. B* **48**, 790-811.
9. Redinbo, M.R., Cascio, D., Choukair, M.K., Rice, D. Merchant, S. & Yeates, T.O. (1992). The 1.5-Ångström crystal-structure of plastocyanin from the green alga *Chlamydomonas reinhardtii*. *Biochemistry* **32**, 10560-10567.
10. Bagby, S., Driscoll, P.C., Harvey, T.S. & Hill, H.A.O. (1994). High-resolution structure of reduced parsley plastocyanin. *Biochemistry* **33**, 6611-6622.
11. Badsberg, U., *et al*., & Ulstrup, J. (1996). Solution structure of reduced plastocyanin from the blue-green alga *Anabaena variabilis*. *Biochemistry* **35**, 7021-7031.
12. Kannt A., Young, S. & Bendall, D.S. (1996). The role of acidic residues of plastocyanin in its interaction with cytochrome *f*. *Biochim. Biophys. Acta* **1277**, 115-126.
13. Niwa, S., Ishikawa, H., Nikai, S. & Takabe, T. (1980). Electron transfer reactions between cytochrome *f* and plastocyanin from *Brassica komatsuna*. *J. Biochem.* **88**, 1177-1183.
14. Beoku-Betts, D., Chapman, S.K., Knox, C.V. & Sykes, A.G. (1985). Kinetics studies on 1:1 electron-transfer reactions involving blue copper proteins. 11. Effects of pH, competitive inhibition, and chromium(III) modification on the reaction of plastocyanin with cytochrome *f*. *Inorg. Chem.* **24**, 1677-1681.
15. Takabe, T. & Ishikawa, H. (1989). Kinetic studies on a cross-linked complex between plastocyanin and cytochrome *f*. *J. Biochem.* **105**, 98-102.
16. Qin, L. & Kostic, N.M. (1992). Electron-transfer reactions of cytochrome *f* with flavin semiquinones and with plastocyanin. Importance of protein–protein electrostatic interactions and of donor–acceptor coupling. *Biochemistry* **31**, 5145-5150.
17. Meyer, T.E., Zhao, Z.G., Cusanovich, M.A. & Tollin, G. (1993). Transient kinetics of electron transfer from a variety of *c*-type cytochromes to plastocyanin. *Biochemistry* **32**, 4552-4559.
18. Takenaka, K. & Takabe, T. (1984). Importance of local positive charges on cytochrome *f* for electron transfer to plastocyanin and potassium ferricyanide. *J. Biochem.* **96**, 1813-1821.
19. Anderson, G.P., Sanderson, D.G., Lee, C.H., Durell, S., Anderson, L.B. & Gross, E.L. (1987). The effect of ethylenediamine chemical modification of plastocyanin on the rate of cytochrome *f* oxidation and P-700$^+$ reduction. *Biochim. Biophys. Acta* **894**, 386-398.
20. Adam, Z. & Malkin, R. (1989). On the interaction between cytochrome *f* and plastocyanin. *Biochim. Biophys. Acta* **975**, 158-163.
21. Gross, E.L., Curtis, A., Durell, S.R. & White, D. (1990). Chemical modification of spinach plastocyanin using 4-chloro-3,5-dinitrobenzoic acid: characterization of four singly-modified forms. *Biochim. Biophys. Acta* **1016**, 107-114.
22. Gross, E.L. & Curtis, A. (1991). The interaction of nitrotyrosine-83 plastocyanin with cytochromes *f* and *c*: pH dependence and the effect of an additional negative charge on plastocyanin. *Biochim. Biophys. Acta* **1056**, 166-172.
23. Christensen, H.E.M., Conrad, L.S. & Ulstrup, J. (1992). Effects on NO_2-modification of Tyr83 on the reactivity of spinach plastocyanin with cytochrome *f*. *Biochim. Biophys. Acta* **1099**, 35-44.
24. He, S., Modi, S., Bendall, D.S. & Gray, J.C. (1991). The surface-exposed tyrosine residue Tyr83 of pea plastocyanin is involved in both binding and electron transfer reactions with cytochrome *f*. *EMBO J.* **10**, 4011-4016.
25. Modi, S., He, S., Gray, J.C. & Bendall, D.S. (1992). The role of surface-exposed Tyr83 of plastocyanin in electron transfer from cytochrome *c*. *Biochim. Biophys. Acta* **1101**, 64-68.
26. Modi, S., Nordling, M., Lundberg, L.G., Hansson, Ö. & Bendall, D.S. (1992). Reactivity of cytochromes *c* and *f* with mutant forms of spinach plastocyanin. *Biochim. Biophys. Acta* **1102**, 85-90.
27. Lee, B.H., Hibino, T., Takabe, T., Weisbeek, P.J. & Takabe, T. (1995). Site-directed mutagenetic study on the role of negative patches on silene plastocyanin in the interactions with cytochrome *f* and photosystem I. *J. Biochem.* **117**, 1209-1217.
28. Morand, L.Z., Frame, M.K., Colvert, K.K., Johnson, D.A., Krogmann, D.W. & Davis, D.J. (1989). Plastocyanin–cytochrome *f* interaction. *Biochemistry* **28**, 8039-8047.

29. Qin, L. & Kostic, N.M. (1993). Importance of protein rearrangement in the electron-transfer reaction between the physiological partners cytochrome *f* and plastocyanin. *Biochemistry* **32**, 6073-6080.
30. Zhou, J., Fernández-Velasco, J.G. & Malkin, R. (1996). N-terminal mutants of chloroplast cytochrome *f*. *J. Biol. Chem.* **271**, 6225-6232.
31. Soriano, G.M., Ponamarev, M.V., Tae, G.-S. & Cramer, W.A. (1996). Effect of the interdomain basic region of cytochrome *f* on its redox reactions *in vivo*. *Biochemistry* **35**, 14590-14598.
32. Pearson, D.C. Jr., Gross, E.L. & David, E.S. (1996). Electrostatic properties of cytochrome *f*: implications for docking with plastocyanin. *Biophys. J.* **71**, 64-76.
33. Ullmann, G.M., Knapp, E.W. & Kostic, N.M. (1997). Computational simulation and analysis of dynamic association between plastocyanin and cytochrome *f*. Consequences for the electron-transfer reaction. *J. Am. Chem. Soc.* **119**, 42-52.
34. Ubbink, M., Lian, L.Y., Modi, S., Evans, P.A. & Bendall, D.S. (1996). Analysis of the ^{1}H-NMR chemical shifts of Cu(I)-, Cu(II)- and Cd-substituted pea plastocyanin. *Eur. J. Biochem.* **242**, 132-147.
35. Keller, R. M. & Wütrich, K. (1972). The electronic *g*-tensor in cytochrome b_5: high resolution proton magnetic resonance studies. *Biochim. Biophys. Acta* **285**, 326-336.
36. Williams, G., Clayden, N.J., Moore, G.R. & Williams, R.J.P. (1985). Comparison of the solution and crystal structures of mitochondrial cytochrome *c*. *J. Mol. Biol.* **183**, 447-460.
37. Emerson, S.D. & La Mar, G.N. (1990). NMR determination of the orientation of the magnetic susceptibility tensor in cyanometmyoglobin: a new probe for steric tilt of bound ligand. *Biochemistry* **29**, 1556-1566.
38. Veitch, N.C., Whitford, D. & Williams R.J.P. (1990). An analysis of pseudocontact shifts and their relationship to structural features of redox states of cytochrome b_5. *FEBS Lett.* **269**, 297-304.
39. Feng, Y., Roder, H. & Englander, S.W. (1990). Redox-dependent structure change and hyperfine nuclear magnetic resonance shifts in cytochrome *c*. *Biochemistry* **29**, 3494-3504.
40. Gao, Y., Boyd, J., Pielak, G.J. & Williams, R.J.P. (1991). Comparison of reduced and oxidized yeast iso-1-cytochrome *c* using proton paramagnetic shifts. *Biochemistry* **30**, 1928-1934.
41. Timkovich, R. & Cai, M. (1993). Investigation of the structure of oxidized *Pseudomonas aeruginosa* cytochrome *c*-551 by NMR: comparison of observed paramagnetic shifts and calculated pseudocontact shifts. *Biochemistry* **32**, 11516-11523.
42. Gochin, M. & Roder, H. (1995). Protein structure refinement based on paramagnetic NMR shifts: applications to wild-type and mutant forms of cytochrome *c*. *Protein Sci.* **4**, 296-305.
43. Zhao, D., Hutton, H.M., Cusanovich, M.A. & Mackenzie, N.E. (1996). An optimized g-tensor for *Rhodobacter capsulatus* cytochrome c_2 in solution: a structural comparison of the reduced and oxidized states. *Protein Sci.* **5**, 1816-1825.
44. Banci, L., Bertini, I., Bruschi, M., Sompornpisut, P. & Turano, P. (1996). NMR characterization and solution structure determination of the oxidized cytochrome c_7 from *Desulfuromonas acetoxidans*. *Proc. Natl. Acad. Sci. USA* **93**, 14396-14400.
45. Banci, L., *et al*., & Turano, P. (1996). The use of pseudocontact shifts to refine solution structures of paramagnetic metalloproteins – Met80Ala cyano-cytochrome *c* as an example. *J. Biol. Inorg. Chem.* **1**, 117-126.
46. Banci, L., *et al*., & Turano, P. (1997). Solution structure of oxidized horse heart cytochrome c. *Biochemistry* **36**, 9867-9877.
47. Banci, L., *et al*., & Gray, H.B. (1997). Pseudocontact shifts as constraints for energy minimization and molecular dynamics calculations on solution structures of paramagnetic metalloproteins. *Proteins* **29**, 68-76.
48. Guiles, R.D., *et al*., & Waskell, L. (1996). Pseudocontact shifts used in the restraint of the solution structures of electron transfer complexes. *Nat. Struc. Biol.* **3**, 333-339.
49. Bertini, I. & Luchinat, C. (1996) NMR of paramagnetic substances. *Coor. Chem. Rev.* **150**, 1-296.
50. Rigby, S.E.J., Moore, G.R., Gray, J.C., Gadsby, P.M.A., George, S.J. & Thomson, A.J. (1988). N.m.r., e.p.r. and magnetic-c.d. studies of cytochrome *f*. *Biochem. J.* **256**, 571-577.
51. Ubbink, M., Campos, A.P., Teixeira, M., Hunt, N.I., Hill, H.A.O. & Canters, G.W. (1994). Characterization of mutant Met100Lys of cytochrome *c*-550 from *Thiobacillus versutus* with lysine-histidine heme ligation. *Biochemistry* **33**, 10051-10059.
52. Ubbink, M. & Bendall, D.S. (1997). Complex of plastocyanin and cytochrome *c* characterized by NMR chemical shift analysis. *Biochemistry* **36**, 6326-6335.
53. Northrup, S.H. (1996). Computer modelling of protein–protein interactions. In *Protein electron transfer* (D.S. Bendall, ed.), pp.69-97, Bios Scientific Publishers, Oxford, UK.
54. Moser, C.C. & Dutton, P.L. (1996). Outline of theory of protein electron transfer. In *Protein Electron Transfer* (Bendall, D.S., ed.), pp. 1-21, Bios Scientific Publishers, Oxford, UK.
55. Beratan, D.N. & Onuchic, J.N. (1996). The protein bridge between redox centres. In *Protein Electron Transfer* (Bendall, D.S., ed.), pp. 23-42, Bios Scientific Publishers, Oxford, UK.
56. Hazzard, J.T., Moench, S.J., Erman, J.E., Satterlee, J.D. & Tollin, G. (1988). Kinetics of intracomplex electron transfer and of reduction of the components of covalent and noncovalent complexes of cytochrome *c* and cytochrome *c* peroxidase by free flavin semiquinones. *Biochemistry* **27**, 2002-2008.
57. Brooks, H.B. & Davidson, V.L. (1994). Free energy dependence of the electron transfer reaction between methylamine dehydrogenase and amicyanin. *J. Am. Chem. Soc.* **116**, 11201-11202.
58. Hazzard, J.T., Rong, S.-Y. & Tollin, G. (1991). Ionic strength dependence of the kinetics of electron transfer from bovine mitochondrial cytochrome *c* to bovine cytochrome *c* oxidase. *Biochemistry* **30**, 213-222.
59. Tiede, D.M., Vashishta, A.-C. & Gunner, M.R. (1993). Electron-transfer kinetics and electrostatic properties of the *Rhodobacter sphaeroides* reaction center and soluble *c*-cytochromes. *Biochemistry* **32**, 4515-4531.
60. Zhou, J.S. & Kostic, N.M. (1992). Photoinduced electron transfer from zinc cytochrome *c* to plastocyanin is gated by surface diffusion within the metalloprotein complex. *J. Am. Chem. Soc.* **114**, 3562-3563.
61. Qin, L. & Kostic, N.M. (1994). Photoinduced electron transfer from the triplet state of zinc cytochrome *c* to ferricytochrome b_5 is gated by configurational fluctuations of the diprotein complex. *Biochemistry* **33**, 12592-12599.
62. Nocek, J.M., *et al.,* & Hoffman, B.M. (1996). Theory and practice of electron transfer within protein-protein complexes: application to the multidomain binding of cytochrome *c* by cytochrome *c* peroxidase. *Chem. Rev.* **96**, 2459-2489.
63. Bendall, D.S. (1996). Interprotein electron transfer. In *Protein Electron Transfer* (Bendall, D.S., ed.), pp. 43-68, Bios Scientific Publishers, Oxford, UK.
64. Zhang, Q., Marohn, J. & McLendon, G. (1990). Macromolecular recognition in the cytochrome *c* - cytochrome *c* peroxidase complex involves fast two-dimensional diffusion. *J. Phys. Chem.* **94**, 8628-8630.
65. McLendon, G. (1991). Electron transfer between bound proteins. In *Metal Ions in Biological Systems.* (Sigel, H & Sigel, A., eds.), Vol. 27, pp. 183-198, M Dekker, New York, USA.
66. McLendon, G. (1991). Control of biological electron transport via molecular recognition and binding: the "Velcro" model. *Struct. Bond.* **75**, 159-174.
67. McLendon, G. & Hake, R. (1992). Interprotein electron transfer. *Chem. Rev.* **92**, 481-490.
68. Bendall, D.S. & Wood, P.M. (1978). Kinetics of electron transfer through higher-plant plastocyanin. In *Photosynthesis '77. Proceedings of the Fourth International Congress on Photosynthesis* (Hall, D.O., Coombs, J. & Goodwin, T.W., eds.), pp. 771-775, The Biochemical Society, London and Colchester, UK.
69. Maniatis, T, Fritsch, E.F. & Sambrook, J. (1982). *Molecular Cloning: A laboratory manual.* Cold Spring Harbor Press, Cold Spring Harbor, NY.
70. Ejdebäck, M., Young, S., Samuelsson, A. & Karlsson, B.G. (1997). Expression of spinach plastocyanin in *Escherichia coli*. *Protein Expr. Purif.* **11**,17-25.
71. Zhang, O.W., Kay, L.E., Olivier, J.P. & Formankay, J.D. (1994). Backbone ^{1}H and ^{15}N resonance assignments of the N-terminal SH3 domain of drk in folded and unfolded states using enhanced-sensitivity pulsed-field gradient NMR techniques. *J. Biomol. NMR* **4**, 845-858.
72. Kraulis, P.J. (1989). ANSIG: a program for the assignment of protein 1H 2D NMR spectra by interactive graphics. *J. Magn. Reson.* **84**, 627-633.
73. Kraulis, P.J., Domaille, P.J., Campbell-Burk, S.L., van Aken T. & Laue, E.D. (1994). Solution structure and dynamics of Ras p21·GDP determined by heteronuclear three- and four-dimensional NMR spectroscopy. *Biochemistry* **33**, 3515-3531.
74. Brünger, A.T. (1992). *X-PLOR 3.1 manual*. Yale University Press, New Haven, CT, USA.
75. Kraulis, P.J. (1991). MOLSCRIPT: a program to produce both detailed and schematic plots of protein structures. *J. Appl. Cryst.* **24**, 946-950.